IEEE Access
Multidisciplinary | Rapid Review | Open Access Journal
IEEE POWER ENERGY SOCIETY SECTION

Received November 24, 2019, accepted December 11, 2019, date of publication December 20, 2019,
date of current version January 6, 2020.

Digital Object Identifier 10.1109/ACCESS.2019.2961134

Field Trial of Coordinated Control of PV and Energy Storage Units and Analysis of Power Quality Measurements

ONYEMA S. NDUKA[1], (Member, IEEE), LINASH P. KUNJUMUHAMMED[2], (Senior Member, IEEE), BIKASH C. PAL[1], (Fellow, IEEE), ANKUR MAJUMDAR[3], (Member, IEEE), YUE YU[1], (Student Member, IEEE), SUMAN MAITI[4], (Member, IEEE), AND ALI R. AHMADI[5]

[1]Control and Power Group, Imperial College London, London SW7 2AZ, U.K.
[2]Power System Group, Mitsubishi Electric Europe BV, London CR0 6BA, U.K.
[3]DEPsys SA, 1070 Lausanne, Switzerland
[4]Department of Electrical Engineering, IIT Kharagpur, Kharagpur 721302, India
[5]Smart Grid Development, UK Power Networks, London SE1 6NP, U.K.

Corresponding author: Onyema S. Nduka (on212@ic.ac.uk)

This work was supported by the UK Power Networks NIA (Network Innovation Allowance) project – NIA_UKPN0021.

ABSTRACT Trends support low voltage distribution networks will soon experience significant uptake of customer-owned low-carbon technology (LCT) devices especially rooftop photovoltaics (PVs) and small-scale energy storage (SSES) systems. This paradigm shift will introduce some significant challenges in modern distribution network planning and operations owing to the temporal nature of modern demand. Therefore, it became relevant to investigate the UK low voltage (LV) network operations considering high uptake of PVs and SSESs through both field measurements and desktop studies. The aim was to validate through field trials, the flexibility benefits of peak demand reduction and reverse power flow mitigation through smart control of customer-owned SSESs. It was shown that peak demand of up to 60% could be achieved in UK distribution network through the smart control of these devices. In tandem with the demand reduction, the study revealed that type-tested SSES power interface units do not pose significant power quality risks even for 100% customer penetration.

INDEX TERMS Ancillary services, coordinated control, distribution networks, low carbon technology, low voltage, photovoltaics, power quality, small-scale energy storage systems.

I. INTRODUCTION

High uptake of rooftop PVs was promoted by government policies and subsidy schemes in several countries in Europe and beyond. Such policies were driven by the quest for economic and environmental concerns such as the need for carbon-emission reduction. In the UK, customers who own renewable distributed generators (DGs) received compensation as high as 12.03 pence/kWh for energy exported to the utility grid as at year 2012 [1], [2]. This is called the feed-in-Tariff (FiT). Surprisingly, the number of customer-owned PVs soon surpassed the target set by the government. This resulted in the reduction of the FiT to less than 5 pence/kWh [1]–[3] and eventually its withdrawal. Consequently, most customers who own PVs are retrofitting their units with Small Scale Energy Storage (SSES). This way, the excess generation from the PV is used to charge the SSES around noontime when PV generation peaks and the energy is subsequently used around the evening period to meet the household demand.

This trend is anticipated to continue both in the UK and other countries especially as the costs of SSES units continue to drop. For instance, as of 2016, about fifty thousand SSES units have been bought in Germany and the forecasts suggest the trend will continue [4]. Moreover, it is argued that certain power quality (PQ) issues associated with PV systems could be mitigated when the PVs are retrofitted with SSES units. Such PQ issues include voltage rise and reverse power flows (RPF). The SSES is considered capable of smoothing the PV generation profile and reducing the peak demand.

The associate editor coordinating the review of this manuscript and approving it for publication was Guangya Yang.

This is in addition to reduction of customer electricity bills as net import from the network is expected to be decreased [5], [6].

Indeed, while several works exist in the literature about PVs and SSES, these units have often been studied separately. In [7], overvoltage occurrence due to rooftop PV system integration into the network was investigated. Also, [8] suggested that urban networks were more likely to be affected by overvoltage problems caused by the rooftop PVs. Similarly, in [9], an aggregated 13kWp rooftop PV system in Lyon, France, was monitored for both steady-state and transient performance. The authors argued that field measurements did not reveal any significant impact on the LV system due to PV integration. Also, this system which had a total of 6 inverters was said to satisfy the statutory harmonic limits except for the violation of the 6th and 8th (even harmonic) limits. Authors suggested that this could have resulted from the inverters being the transformerless type.

Similar measurement on a 440kWp (60 PV systems and 160 inverters) integrated into an urban LV network in Germany was conducted in [10]. Results revealed that overvoltages existed as well as harmonics but these were negligible. Nevertheless, significant phase imbalance due to the PV integration was noticed [10]. Furthermore, [11], [12] have also studied the harmonic emissions from PVs in networks with significant background distortions and voltage imbalance.

Some publications have also considered the hybrid (i.e. PV and SSES) system in their analysis but the field trials to demonstrate the practicality are still relatively at an early stage. The motivation has always been to improve the network performance with alternative non-network solutions like SSES integration in networks with high rooftop PV penetration. Obviously, network solutions such as reconfiguration, load balancing, transformer and cable upgrade etc are expensive and time consuming and therefore the preference for non-network solutions.

Of course, installing household rooftop PVs and SSESs can be expensive too but this cannot be compared with the financial investments and time which are required for transformer and/or cable replacements. Moreover, the customers who participated in the field trial and as described in this paper already had rooftop PV systems installed. These PVs were simply retrofitted with the SSESs. Consequently, it was simply a matter of the DNO leveraging on the flexibility service available at the customer household while rewarding such customers in return for the ancillary services support.

Existing learnings on hybrid (PV and SSES) systems include those of [5] and [13] where dynamic charge/discharge rate of SSES and coordinated control of utility assets with distributed PV and SSES units were respectively proposed. In [14], the use of PV and SSES for reducing the net power imported from the utility grid was formulated and solved as an optimisation problem. Results indicated 13% reduction in electricity bills for a customer with SSES and PV units.

Ref. [15] has presented the benefits and challenges that resulted from the deployment of behind the meter storage units for the improvement of network performance in Australia. Obviously, several national and international standards exist for the impact assessments. In the UK, statutory requirements - EREC G83 and G5/4-1, are usually used to assess the compliance or violation of these devices' integrations with the distribution network operators (DNOs) requirements [9], [16]. This way, adverse impacts on the network are mitigated.

In addition to the theoretical works, several field trials exist both in the UK and beyond [6], [15], [17]–[19]. An example field demonstration project in the literature is that of [20], which investigated how SSES could be used to smoothen PV generation profile, reduce peak demand and Reverse Power Flow (RPF). Ten customers participated in the trial and the summer and winter periods were the focus of the trial. Field tests were conducted for few days and data extrapolated for other periods of the year in order to develop computational models for simulations.

Furthermore, in [17], modular units (with PVs, batteries and communication devices) were installed in 250 different locations including residential and commercial buildings. It was demonstrated how the SSES and the PVs could provide ancillary services to the network. The company responsible for that trial project argued that since bulk of the UK peak demand resulted from residential loads, it made sense to reduce demand levels through customer owned PV and SSES operation and control.

Another LV-network project on PV and SSES is documented in [18]. That project investigated if there was a business case for using customer-owned PVs and SSES as an alternative to network expansion; 26 residential houses, 5 schools and one office building were used for the trial. These buildings were fitted with PVs, SSESs and communication and control systems. The PV and SSES units were dc-coupled and hence each test site had one power converter which was aimed at reducing harmonic levels. The project findings revealed that the financial gain to the utility was very small but other benefits to customers such as backup power supply could be an attraction. Also, it was admitted that the sample size was small and results could be different with larger size. With such sample size, no known network limits were observed to be exceeded. Nevertheless, it was suggested that higher sample size should be trialled to ascertain clearly what adverse impacts could result in the network due to the SSES and PV proliferation.

While other energy storage projects continue in the UK and beyond, it is pertinent to state at this juncture that the scope of this work is only on LV single-phase connected customer-owned PV systems retrofitted with SSES. The aim was to investigate using larger sample size of customer households with PV and SSES, the impacts of these units on a typical UK LV distribution network operating performance. In particular, the trial sought to investigate if there was need for the revision of statutory limits such as EREC G83. It was also aimed at establishing through field trials if the coordinated control of a large number of customer-owned PV and SSES units connected to the network could be used to reduce the peak demand and thus defer utility asset upgrade. SSES capability to mitigate RPF was also assessed practically.

To this end, 70 customers in South East England were selected and their PV units retrofitted with SSES. The customer PVs were rated 2 - 4kWp while the SSES maximum charge and discharge powers were respectively 1.2kW and 1.6kW. Smart meters were also installed to capture both the power and harmonic frequency information. The trial was conducted for a total of 12-months in order to cover the effects of seasonal variations. Data realised were timestamped and had interval of one second. The data management was carried out using SQLite while data mining, cleansing and analysis were conducted using Python and MATLAB.

Twenty-three quantities were measured including the active and apparent powers, power factor, frequency and the voltages and currents at power and harmonic frequencies. The measurements were obtained for each of the SSES, PV and the mains meter. Hence, data having 23 columns (indices) and 86400 rows (seconds) for each device were realised per day. That is for a typical day, $23 \times 86400 \times 3$ data format was obtained. These data were uploaded directly to Imperial College London repository and processed using a dedicated workstation. The field data were further deployed in desktop studies in order to investigate scaled-up levels of penetration.

To comply with general data protection rights (GDPR), the customer data were anonymised. Hence, we refer to each customer simply as house W_i where W_i is a value that has been assigned by the stakeholders in the project.

Furthermore, it is pertinent to state that although the field trial was conducted on a UK LV network, the findings in this paper are useful to several stakeholders, especially DNOs in European nations. This is because the UK LV system is like the networks in other EU countries. Moreover, even for a system with entirely different characteristics from representative European systems, our findings will provide useful information upon which field trials for such systems could be built upon.

In addition to Section I, other sections of this paper are presented as follows: Section II describes the field monitoring and data acquisition whereas Section III highlights the results of the data analytics in the context of peak demand reduction following the coordinated control of the SSES units. Alongside the validation of the ancillary service provision of the PV and SSES, in Section IV, the PQ field data are analyzed and discussed. Next, the desktop simulation studies are presented in Section V and thereafter is the conclusion of this technical work.

II. DESCRIPTION OF FIELD MONITORING

The field trial schematic diagram is as shown in Figure 1. Three sensors (power quality meters (PQM)) were connected at the output terminals of the PV, SSES and the mains at the customer premises as shown in the diagram. The default

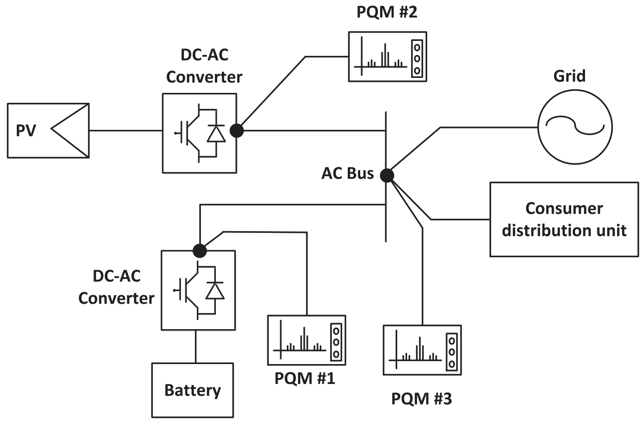

FIGURE 1. Field demonstration - AC connected system [21].

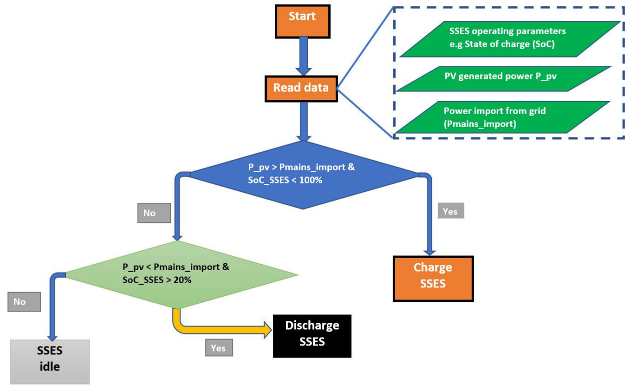

FIGURE 2. SSES default charge/discharge algorithm.

operation was such that a customer's demand was met by the generation from PV and the excess output power used to charge the battery. In other words, the SSES began to charge when it was detected that customer's demand had been fully met and power been fed back into the grid. On the other hand, SSES discharged when it was observed that power was drawn from the grid and the batteries still had adequate stored energy from previous charging periods.

The logical sequence for the charge and discharge operations of the SSESs can be summarised by the flowchart in Figure 2.

III. PEAK DEMAND REDUCTION BY COORDINATED CONTROL OF DECENTRALISED PV AND SSES SYSTEMS

As highlighted previously, the default goal of each household with the SSES installed was to reduce the net power imported from the grid, thereby reducing the costs of electricity bills. To achieve this aim, the customer charged the SSES from the excess PV generation during peak output hours - usually around noon and subsequently discharged the SSES at evening demand periods.

To assess the effectiveness of the default method in reducing the customer demand for the four seasons in the UK - autumn, spring, winter and summer, the demand

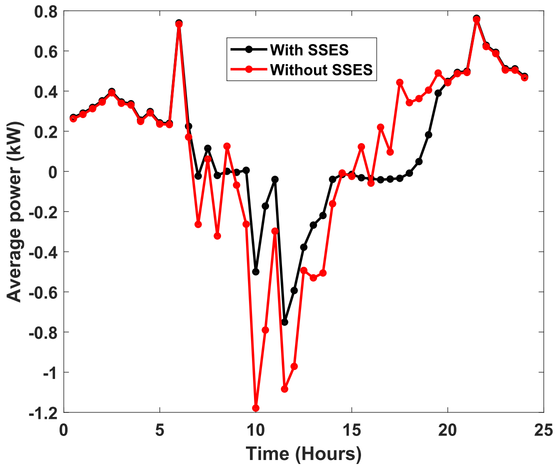

FIGURE 3. Example profile for summer month for House #16.

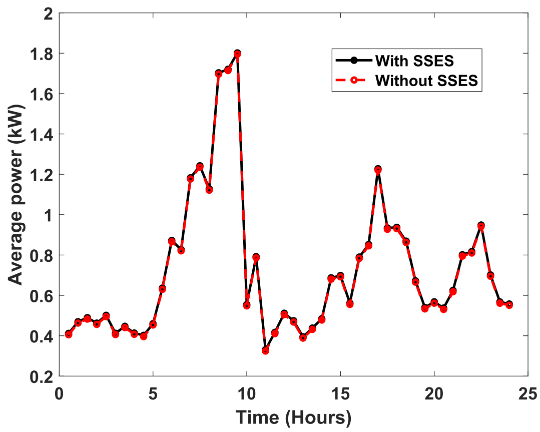

FIGURE 4. Example profile for winter month for a House #16.

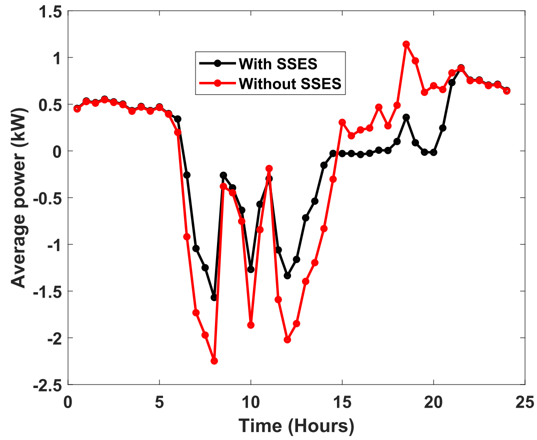

FIGURE 5. Example spring day profile for house #16.

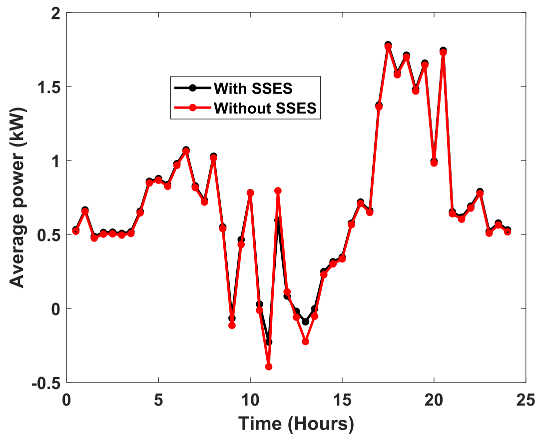

FIGURE 6. Example autumn day profile for house #16.

profiles were plotted based on the one-year field measurements. Indeed, different seasons were considered as it is common knowledge that electrical load profiles are influenced by weather and seasonal variations. For instance, customers use more of their heating appliances during the cold winter periods than the summer. Obviously, this would influence the load pattern for both seasons.

As most of the households showed similar trend, only the plots for one of the houses are shown for illustration. Figures 3 and 4 respectively denote the profiles for the summer and winter periods. For completeness, the spring and autumn profiles are also shown in Figures 5 and 6. Clearly, Figures 3 and 5 show that the SSES helped significantly to lower the RPFs as well as the evening peak demand - this is obvious when the red and black lines in the plots are compared. However, in Figure 4, the household's profile with and without the SSES were the same. A further examination of the charge and discharge power of the SSES during the winter period showed that the SSESs were mostly idle at this period of the year. This is because the SSES were not adequately charged as the solar irradiance level (as well as PV generation) was low and thus the SSESs could not discharge during the customer's evening peak demand.

This therefore revealed clearly that some form of smart control was needed for the customer as well as the DNO to optimally use the SSES all year round. The idea is that if a strong case is proven for use of customer-owned assets for ancillary services, then, DNO's can develop necessary incentives or financial rewards for this flexibility services.

Consequently, the firmware of some selected SSESs were re-programmed by the industry partner, such that the units could charge from off the grid or discharge to supply household demand upon receiving a control signal from a remote location (from the DNO). This was referred to as active-control trial (ACT) in the field demonstration. During the field trial, the control signals were activated at some pre-defined times based on a priori knowledge of the DNO's network profiles. The time-schedule is as shown in Figure 7.

The ACT was conducted for 21-days and during a winter (February) month. The forced charge and forced discharge in Figure 7 respectively denote a selected group of SSES units charging from off the grid and discharging to offset the network demand at the set times. This control scheme overrides the default operation of the SSESs.

The aggregated demand profile for 12 selected houses which participated in the ACT is as shown in Figure 8. The percentage reduction in peak demand for these aggregated

Date	Start forced charge	Stop forced charge	Force charge duration	Start forced discharge	End forced discharge	Discharge duration
5/2/2018	1:00	4:30	3:30	17:30	18:00	0:30
6/2/2018	1:30	4:30	3:00	17:30	18:00	0:30
7/2/2018	1:30	4:30	3:00	18:00	18:30	0:30
8/2/2018	2:30	7:30	5:00	18:00	18:30	0:30
9/2/2018	2:30	7:30	5:00	18:30	19:00	0:30
10/2/2018	2:00	7:30	5:30	18:30	19:00	0:30
11/2/2018	2:00	5:00	3:00	19:00	19:30	0:30
12/2/2018	2:00	5:00	3:00	17:00	18:00	1:00
13/2/2018	2:00	5:00	3:00	17:00	18:00	1:00
14/2/2018	2:30	7:00	4:30	18:00	19:00	1:00
15/2/2018	2:30	7:00	4:30	18:00	19:00	1:00
16/2/2018	2:30	7:00	4:30	19:00	20:00	1:00
17/2/2018	2:30	7:00	4:30	20:00	21:00	1:00
18/2/2018	2:30	7:00	4:30	20:00	21:00	1:00
19/2/2018	2:30	7:00	4:30	17:30	18:30	1:00
20/2/2018	2:30	7:00	4:30	17:30	18:30	1:00
21/2/2018	2:30	7:00	4:30	18:30	19:30	1:00
22/2/2018	2:30	7:00	4:30	17:30	19:00	1:30
23/2/2018	2:30	7:00	4:30	18:00	19:30	1:30
24/2/2018	2:30	7:00	4:30	18:30	20:00	1:30
25/2/2018	2:30	7:00	4:30	19:00	20:30	1:30

FIGURE 7. Active control trial schedule.

households is also shown in Figure 9. This plot clearly revealed that an average of 58% reduction in peak demand per household could be achieved from the ACT. This implies significant financial savings and deferral of network expansion for the utility. Thus, it has been proven that the DNO can leverage on customer-owned assets for providing ancillary services, especially peak demand reduction to the network.

A further task was to analyse if the SSES units responded to the control signals in a reasonable time frame. This was checked against the recommended response limit in [22]. The field data showed that the average response rate for the SSES was 87%. It was anticipated that success rate of 100% could be achieved by the use of improved communication medium. The project demonstration used the WiFi connection available at customer premises and this in some cases became unreliable or weak. This therefore advocates the relevance of strong communication link for such trials.

IV. POWER QUALITY MONITORING AND VALIDATION WITH EREC G83 AND G5/4-1

As highlighted previously, this technical work was also aimed at investigating if significant uptake of SSESs into the LV distribution network would pose any PQ risk to the network especially in the context of harmonic pollution. Moreover, there was need to understand if the "EREC G83 standard" [9] was adequate for SSES proliferated networks or whether there was a need for revision. This is because by standard, DNOs are not required to monitor the installation of DGs at customer premises that are ≤ 16A/phase [16].

Also, it was desired to examine to what extent the RPF issues associated with rooftop PVs could be reduced with the integration of SSESs. To verify these hypotheses, the field data acquired from the sensors installed in the various households were analyzed.

A. REVERSE POWER FLOW ANALYSIS

Figure 10 is an equivalent representation of aggregation of instances where power was still exported back to the grid despite some of the PV power generation been used for charging of the SSES units.

A thorough observation of the maximum PV output powers and the maximum charging powers of the SSESs at these households revealed that the SSESs capacities were lesser than those of the PVs. Therefore, the SSESs were fully charged in quicker than expected time and thus, RPF could not be completely avoided. Indeed, this is not a serious concern, as modern LV networks tolerate some levels of RPFs except when the quantum and duration violate the standard limits [23]. Moreover, higher levels of RPFs would have occurred had the SSESs not been installed in the customer premises at all.

B. NET GENERATION FROM COMBINED PV AND SSES OPERATION

In accordance with EREC G83, the superposed net generation from the customer-owned PV and SSES units were assessed against the 16A/phase limit [16]. Where the net generation at the customer premise is ≤ 16A/phase, then that customer is compliant, otherwise, a violation is recorded. A plot of the households where the latter was observed is as shown in Figure 11. Clearly, House #17 had the highest times where net generation at the customer end exceeded 16A/phase. A further inquiry revealed that this customer was already known and registered with the DNO as "EREC G59" [24] compliant and therefore was not required to satisfy the EREC G83. Put differently, EREC G59 customers can have generation that exceed 16A/phase.

C. HARMONIC DATA ANALYSIS

The harmonic data of the SSESs were analyzed for the different houses. The assessment was done in accordance with the procedure recommended in EREC G83 [9] and using the harmonic indices provided in the Appendix. The plots showing the percentage of times the 3rd and 5th harmonic emissions violated the limits are as plotted in Figures 12 and 13.

Summarily, approximately 16% of the houses involved in the trial had SSES that in some instances had third harmonic values greater than expected. Also, 11% households were seen to have the fifth harmonic level exceeded at some instances. The other harmonic orders were not very significant. Another observation realised from the harmonic data is that the PV power converter performed better than the SSES converter in terms of harmonic emissions. This is as illustrated in Figure 14.

Also, Figure 14 shows that the harmonic emissions from the PV and SSES were within the limits; interestingly, the level of emissions observed at the mains meter exceeded the statutory requirements. This therefore revealed that there existed background harmonics due to other nonlinear loads.

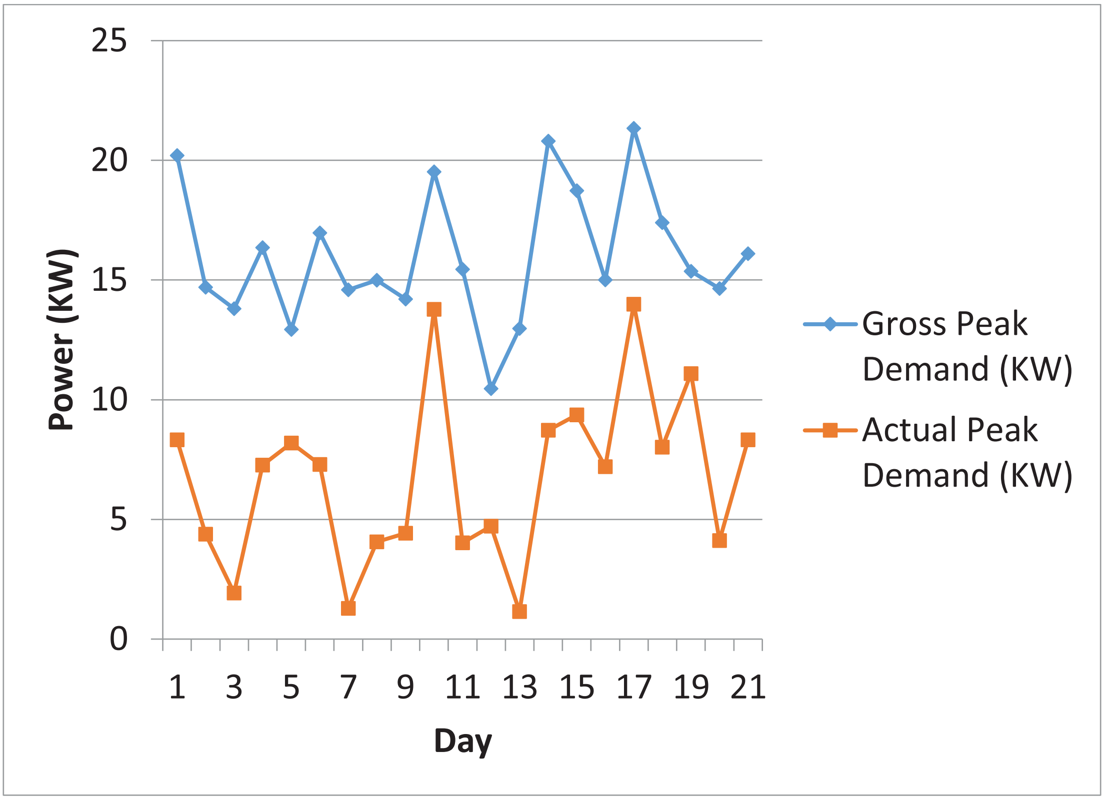

FIGURE 8. Aggregated demand profile with and without ACT.

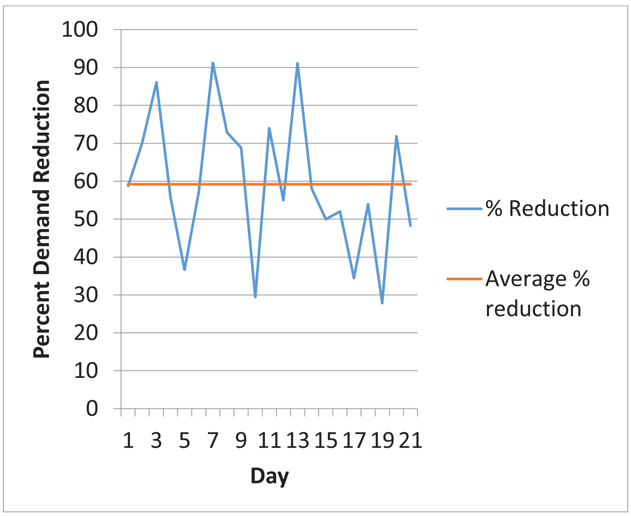

FIGURE 9. Percentage peak demand reduction through ACT.

To ascertain this, a customer nonlinear load ownership survey was conducted and the results showed that the customer devices comprised of such appliances as was predicted. This is as shown in Figure 15. Comparing Figures 12 and 15 show that House #5 which had the most significant SSES third harmonic emission actually had harmonic distorting loads like electric vehicle (EV), LED lamps, desktop computer etc. It is likely that interactions between the SSES unit and the harmonic distorting loads could have led to instances where SSES harmonic data were higher than expected. These interactions are also likely to be the case for other households with SSESs that had higher than expected fifth harmonic levels.

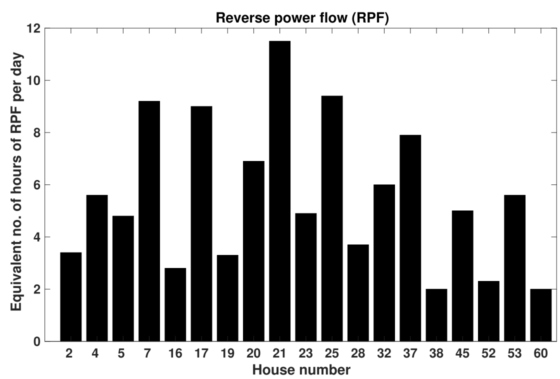

FIGURE 10. Average duration of reverse power flow to grid (hrs/day) for July 2017.

D. STATISTICAL ANALYSIS OF HARMONIC DATA

A statistical analysis was conducted to investigate if the harmonic currents from the PV and SSES converters in any way correlate with the harmonic voltages at the mains. This was done using correlation analysis. Specifically, the Spearman's correlation coefficient was used as it is well known that

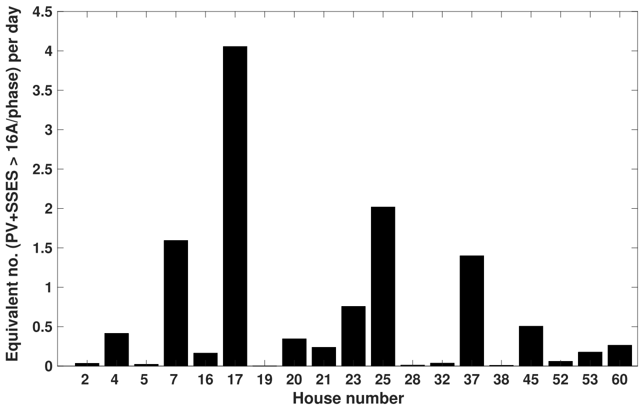

FIGURE 11. Investigation of compliance/violation with EREC G83 16A/phase requirement.

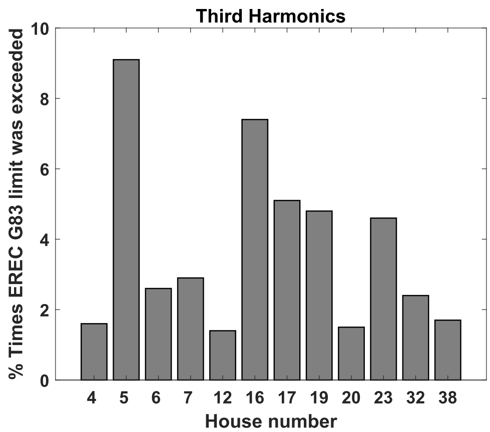

FIGURE 12. Plot of summary of SSESs third harmonic limit compliance with EREC G83.

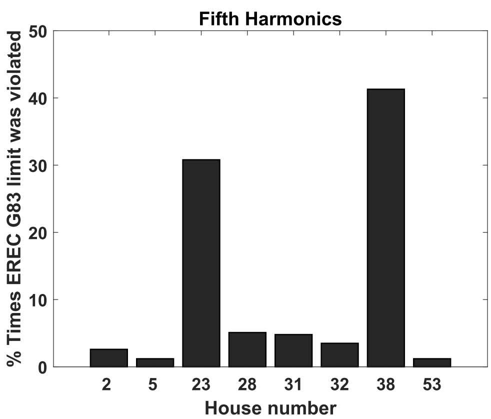

FIGURE 13. Plot of summary of SSESs fifth harmonic limit compliance with EREC G83.

Pearson's approach is very sensitive to outliers [25]. Readers interested to gain further insights into correlation analysis and the use of Spearman's approach are referred to [25].

The scatter plots for the 3rd and 5th harmonic current datasets of the SSES versus the corresponding mains harmonic voltage dataset of House #23 for a day in month of July are shown in Figure 16. The Spearman's correlation coefficient realised for the above 3rd and 5th harmonic order

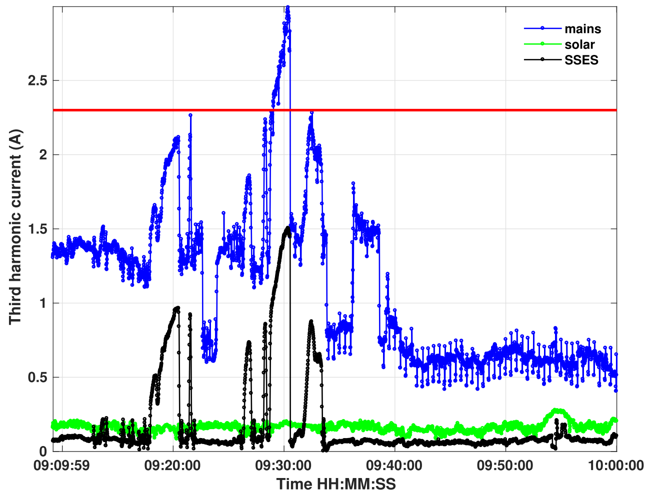

FIGURE 14. Example third harmonic current data of PV, SSES and mains analyzed for House #23.

	Nonlinear load type							
House No	UPS	EV	Heat pump	Boiler	LED	Desktop computer	Laptop	Printer
1	x	x	x	x	Yes	x	Yes	x
2	x	x	Yes	x	Yes	Yes	Yes	x
3	x	x	x	Yes	Yes	x	Yes	x
5	x	Yes	x	x	Yes	Yes	Yes	x
6	x	x	x	x	Yes	Yes	Yes	x
7	x	x	x	x	Yes	x	Yes	x
8	x	x	x	x	Yes	Yes	Yes	x
12	x	x	x	x	Yes	x	x	x
14	x	x	x	Yes	Yes	Yes	Yes	x
15	Yes	x	x	x	x	Yes	Yes	x
17	Yes	x	x	x	Yes	Yes	Yes	x
19	Yes	Yes	x	x	Yes	Yes	Yes	x
20	x	x	x	x	Yes	Yes	Yes	x
22	x	x	x	x	Yes	Yes	Yes	x
23	Yes	Yes	x	x	Yes	Yes	Yes	x
25	x	x	x	x	Yes	Yes	Yes	x
26	x	Yes	x	x	Yes	Yes	Yes	Yes
31	x	Yes	x	x	Yes	Yes	Yes	x
37	x	Yes	x	x	Yes	x	Yes	x
41	x	Yes	x	x	Yes	x	Yes	x
47	x	Yes	x	x	Yes	Yes	Yes	x
53	x	Yes	x	x	Yes	x	Yes	x
60	x	Yes	x		Yes	Yes	Yes	x
	x: means not present or the anwer was not provided by the customer							

FIGURE 15. Surveyed nonlinear loads at customer premises.

plots are respectively 0.3951 and 0.1890. Also, the corresponding p-value was 0.0000 for both harmonic orders.

For completeness, Figure 17 is the heatmap showing the result of the correlation analyses for House #23 based on 2-weeks datasets. The different bandwidths of harmonics have been considered as shown in the heatmap. Clearly, the heatmap suggests that the third and the seventh harmonic currents of the SSES influence the third and seventh harmonic voltages that exist at the mains. The other harmonic orders did not reveal noticeable correlation as seen in the figure.

For clarity, a clustering approach that took into account the different operational states of the devices was applied to the datasets and the correlation analysis re-evaluated. From practical experience, we considered six possible combinations of the simultaneous operations of the PV and SSES and these have been grouped into cases as shown in Figure 18.

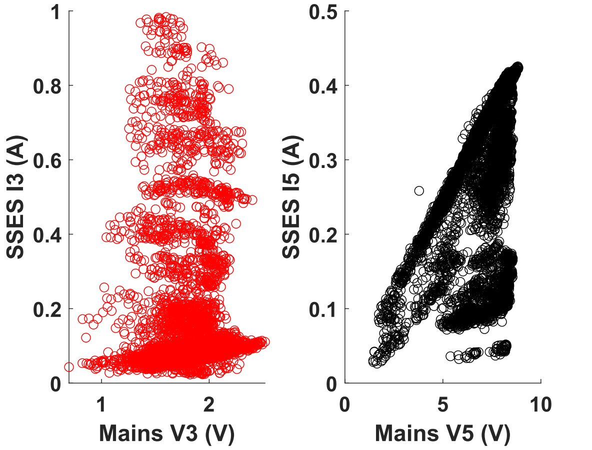

FIGURE 16. Scatter plot of SSES harmonic currents and mains harmonic voltages for House #23.

Date	Bandwidth of harmonics					
	h2	h3	h4	h5	h6	h7
17/07/2017	0.0915	0.6155	-0.039	-0.0302	-0.0021	0.5778
18/07/2017	0.0539	0.5607	-0.031	0.1973	0.0176	0.4684
19/07/2017	0.0359	0.7133	0.0258	0.0315	-0.0535	0.6104
20/07/2017	0.0948	0.6725	0.0257	0.0796	0.0206	0.4573
21/07/2017	0.0936	0.4784	-0.0023	0.0248	-0.0512	0.4744
22/07/2017	0.0383	0.4033	-0.0166	0.359	0.0656	0.4013
23/07/2017	0.1504	0.5617	0.1624	0.0128	0.1107	0.3834
24/07/2017	0.0268	0.4678	0.0236	0.002	0.0161	0.3934
25/07/2017	0.0449	0.3993	-0.0191	-0.0312	0.0222	0.5078
26/07/2017	0.1214	0.5907	0.0222	0.0805	-0.0282	0.5417
27/07/2017	0.0002	0.5236	-0.0635	0.0617	-0.0733	0.6423
28/07/2017	0.0689	0.5757	-0.0472	0.0589	-0.0505	0.5781
29/07/2017	-0.0113	0.4455	0.0872	0.1031	-0.0092	0.5787
30/07/2017	0.0543	0.3951	0.0352	0.189	0.0634	0.4515

FIGURE 17. Heatmap of the correlation analysis for 2-weeks dataset of House #23.

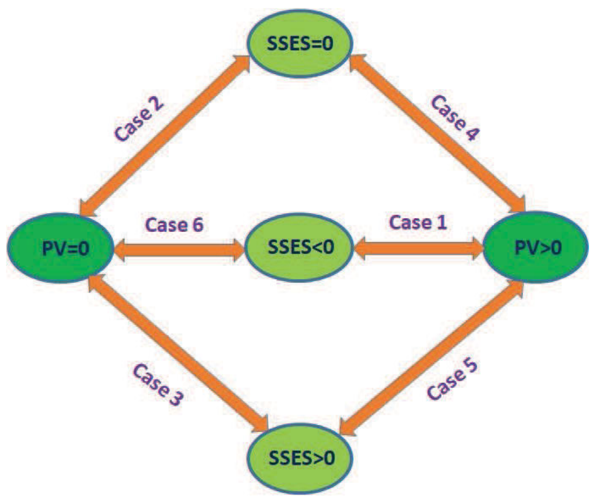

FIGURE 18. Possible scenarios of combined PV and SSES operations.

In case 1, the PV generates power whereas the SSES is in charging state while case 2 involved zero PV generation and idle SSES operation. Similarly, cases 3 and 4 respectively denote zero PV generation and SSES discharging and PV generating power and idle SSES operation. Lastly for cases

Charging						
Date	Bandwidth of harmonics					
	h2	h3	h4	h5	h6	h7
17/07/2017	0.0501	0.2662	-0.0257	0.6924	0.0508	0.6304
18/07/2017	0.1468	0.4457	0.1299	0.6237	0.19	0.6762
19/07/2017	0.0628	0.4391	0.061	0.5766	-0.0968	0.7761
20/07/2017	0.0899	0.4104	0.0853	0.5064	0.0353	0.7663
21/07/2017	0.076	0.0265	0.0286	0.5432	0.0197	0.7244
22/07/2017	0.0899	0.4104	0.0853	0.5064	0.0353	0.7663
23/07/2017	-0.0454	0.2506	-0.0769	0.8932	0.2038	0.8596
24/07/2017	0.1271	0.3431	0.0517	0.3839	0.1438	0.5583
25/07/2017	-0.0757	0.3639	-0.1139	0.653	0.0188	0.6004
26/07/2017	0.1619	0.3678	0.1727	0.6662	0.0725	0.6694
27/07/2017	-0.0308	0.4937	-0.0647	0.6274	-0.0712	0.6755
28/07/2017	0.0334	0.469	-0.0901	0.6808	-0.0815	0.7173
29/07/2017	0.03	0.4113	-0.003	0.5788	-0.0179	0.5913
30/07/2017	0.0282	0.3422	0.0372	0.4887	0.0587	0.5265

FIGURE 19. Heatmap of the correlation analysis - charging mode.

Discharging						
Date	Bandwidth of harmonics					
	h2	h3	h4	h5	h6	h7
17/07/2017	0.2219	0.036	0.0407	0.6855	0.1241	0.6009
18/07/2017	-0.1184	-0.1321	-0.1945	0.6174	-0.1356	0.5603
19/07/2017	0.1374	0.2158	-0.0295	0.593	-0.0705	0.6414
20/07/2017	0.0886	0.0821	-0.0815	0.6376	-0.0151	0.7677
21/07/2017	-0.0445	-0.0551	-0.1589	0.9588	-0.1912	0.6941
22/07/2017	0.0886	0.0821	-0.0815	0.6376	-0.0151	0.7677
23/07/2017	0.0314	0.0358	0.0484	0.2599	0.2155	0.06
24/07/2017	0.0014	0.0466	0.0162	0.7071	0.0264	0.4337
25/07/2017	0.1627	-0.3392	0.0035	0.8479	0.1224	0.4495
26/07/2017	0.1508	0.2105	-0.0259	0.9543	-0.0358	0.8841
27/07/2017	0.3055	-0.045	0.0209	0.7453	-0.0017	0.5608
28/07/2017	0.0195	-0.0895	-0.1073	0.8604	0.0202	0.5945
29/07/2017	-0.0566	0.231	0.0587	0.2896	-0.032	0.5
30/07/2017	0.0538	-0.0974	-0.0306	0.5725	0.0737	0.2956

FIGURE 20. Heatmap of the correlation analysis - discharging mode.

5 and 6, while the former involved PV generating and SSES discharging, the latter involved zero PV generation and SSES charging from off the grid. This clustering became relevant in order to accurately evaluate the contributions of the PV and SSES harmonic emissions to distortion in the mains voltage.

Repeating the Spearman's correlation analysis taking into account two of the above mentioned scenarios - SSES mostly in charging mode (case 6) and SSES mostly discharging to offset customer evening demand (case 3), two heatmaps are as shown in Figures 19 and 20.

The clustering approach revealed that for both charging and discharging operations of the SSES, the fifth and seventh harmonic currents were more correlated to the corresponding harmonic mains voltages than the third harmonic current. This observation was previously concealed without the clustering approach.

V. DESKTOP SIMULATION WITH FIELD DATA

In order to scale up the number of SSESs in the network, a desktop study was conducted. Particularly, power flows and harmonic load flow studies were simulated using the

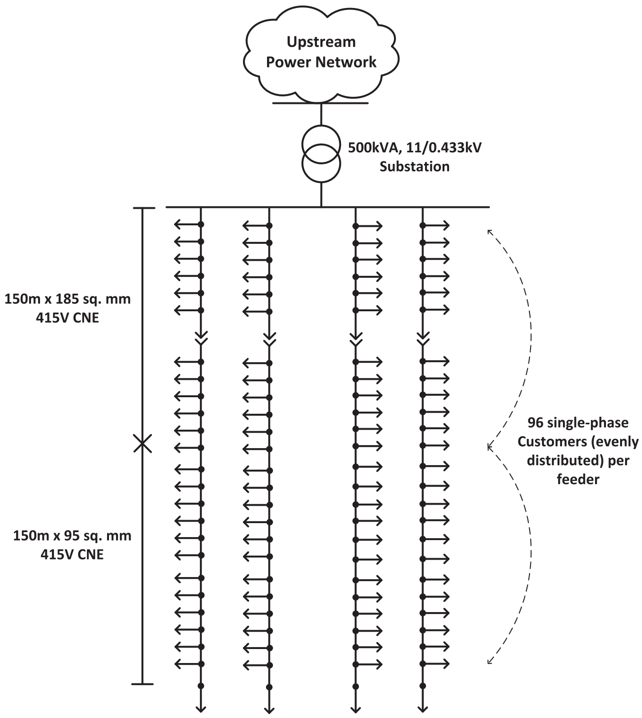

FIGURE 21. Representative UK LV distribution network.

DigSILENT PowerFactory software [26]. The test UK LV distribution network used for simulations had 4 outgoing feeders from the 500kVA substation transformer. The total number of customers connected to the LV network was 384 with 96 single-phase customers connected to each outgoing feeder. The customers were supplied power through underground cables; the parameters and other details of the test network are as obtained from [27] and provided in the Appendix. Figure 21 shows the test power system.

A. SYSTEM-LEVEL ASSESSMENT OF THE IMPACTS OF COORDINATED SSES CONTROL ON TRANSFORMER LOADING

The impact of coordinated control of SSES was investigated on a system-level by assessing the transformer loading levels with and without the activation of the ACT. That is, field data for load profiles without and with ACT were used in the power flow analysis study implemented using a commercial software - DigSILENT PowerFactory [26].

The current injection method [28], [29] of power flow analysis was adopted in this study. This is mathematically formulated as written below [28], [30], [31].

$$\begin{bmatrix} \triangle I_{i_1} \\ \triangle I_{r_1} \\ \triangle I_{i_2} \\ \triangle I_{r_2} \\ \triangle I_{i_3} \\ \triangle I_{r_3} \\ \vdots \\ \triangle I_{i_m} \\ \triangle I_{r_m} \end{bmatrix} = \begin{bmatrix} Y_{11}^* & Y_{12}^* & \ldots & Y_{1m}^* \\ Y_{21}^* & Y_{22}^* & \ldots & Y_{2m}^* \\ Y_{31}^* & Y_{32}^* & \ldots & Y_{3m}^* \\ \vdots & \vdots & \vdots & \vdots \\ Y_{m1}^* & Y_{m2}^* & \ldots & Y_{mm}^* \end{bmatrix} \begin{bmatrix} \triangle V_{r_1} \\ \triangle V_{i_1} \\ \triangle V_{r_2} \\ \triangle V_{i_2} \\ \triangle V_{r_3} \\ \triangle V_{i_3} \\ \vdots \\ \triangle V_{r_m} \\ \triangle V_{i_m} \end{bmatrix} \tag{1}$$

where:

$$Y_{nn}^* = \begin{bmatrix} A_{11} & A_{12} \\ A_{21} & A_{22} \end{bmatrix}; \quad Y_{mn}^* = \begin{bmatrix} B_{mn} & G_{mn} \\ G_{mn} & -B_{mn} \end{bmatrix} \tag{2}$$

The terms: A_{11}, A_{12}, A_{21} and A_{22} are defined in the Appendix while the G_{mn} and B_{mn} terms respectively denote the conductance and susceptance of the line, $m-n$. Note that all nodes downstream the substation transformer are considered as constant power nodes in the power flow analysis and have been modelled using the ZIP model [26], [28], [32] as shown in (3).

$$\begin{aligned} \frac{P}{P_0} &= a_p + b_p V + c_p V^2 \\ \frac{Q}{Q_0} &= a_q + b_q V + c_q V^2 \\ a_p + b_p + c_p &= 1 \\ a_q + b_q + c_q &= 1 \end{aligned} \tag{3}$$

where P, Q and V respectively denote the active and reactive powers and the voltage. The a, b and c terms are multipliers with values depending on the type of load.

As highlighted previously, the power flow was implemented with DigSILENT Powerfactory software. Figure 22 shows the reduction in transformer loading following the peak shaving service realised from the coordinated control of the SSES discharge. That is, from the power flow analysis computation, for 100% SSESs uptake, the reduction in peak demand at the transformer secondary was up to 60%. This was based on each controlled SSES meeting 58% of the household demand at the studied period when the active control was activated as was discussed in Section III. Note that the transformer was considered to be operating at maximum base loading level in the simulation before the SSES integration as shown in the Figure 22.

B. HARMONIC LOAD FLOW ANALYSIS

Furthermore, to assess on a system level whether the statutory harmonic limits were met in the network, a harmonic load flow analysis was conducted in DigSILENT PowerFactory software based on IEC 61000-3-6 [26]. The mathematical formulation for the harmonic assessment is given as in (4) [33], [34].

$$\begin{bmatrix} I_1 \\ I_2 \\ I_3 \\ \vdots \\ I_{n-1} \\ I_n \end{bmatrix}_{(h)} = \begin{bmatrix} Y_{11} & Y_{12} & \ldots & Y_{1n} \\ Y_{21} & Y_{22} & \ldots & Y_{2n} \\ Y_{31} & Y_{32} & \ldots & Y_{3n} \\ \vdots & \vdots & \vdots & \vdots \\ Y_{n-1,1} & Y_{n-1,2} & \ldots & Y_{n-1,n} \\ Y_{n1} & Y_{n2} & \ldots & Y_{nn} \end{bmatrix}_{(h)} \begin{bmatrix} V_1 \\ V_2 \\ V_3 \\ \vdots \\ V_{n-1} \\ V_n \end{bmatrix}_{(h)} \tag{4}$$

where h denotes the h^{th} harmonic. The nonlinear loads have been modelled as current sources based on the summation law [26]. That is, the net harmonic current injection is

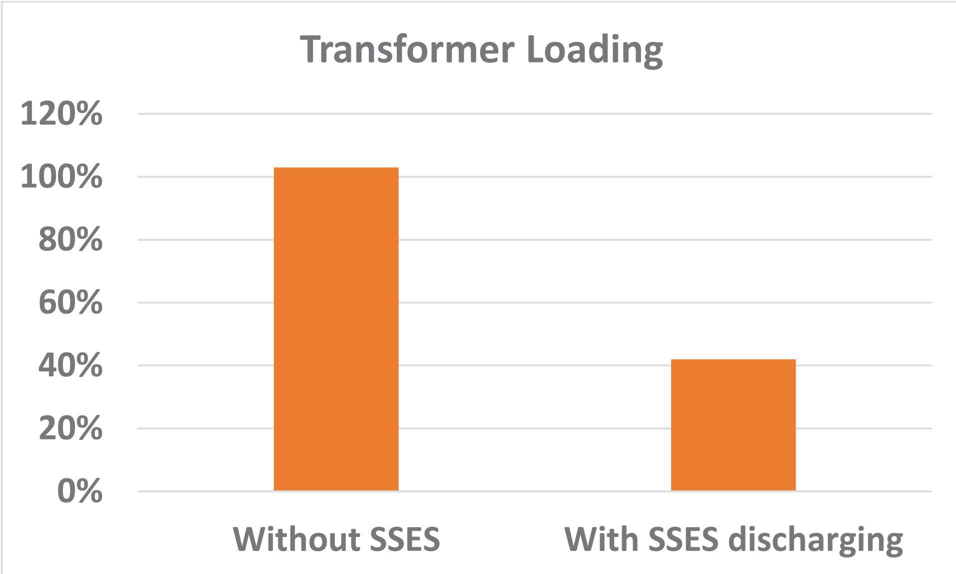

FIGURE 22. Secondary transformer peak demand reduction through coordinated SSESs discharge.

TABLE 1. IEC 61000-3-6 summation exponents [35]–[37].

Exponent value (α)	Harmonic order
1	$h < 5$
1.4	$5 \leq h \leq 10$
2	$h > 10$

obtained as [26], [35], [36]:

$$I_h = \left(\sum_{k=1}^{NK} I_{h,k}^{\alpha} \right)^{\frac{1}{\alpha}} \tag{5}$$

where α is called the harmonic exponent with typical values as shown in Table 1. k refers to the k^{th} harmonic source. Note that the variables to be computed in the formulation in (4) are the harmonic voltages ie: $\left[V_1 \ V_2 \ V_3 \ V_4 \ \ldots \ V_n\right]_{(h)}^{T}$. For the simulation of the harmonic load flow analysis, two scenarios (Scenario 1 and Scenario 2) have been considered.

1) DESCRIPTION OF HARMONIC LOAD FLOW SCENARIOS

As highlighted previously, the test cases for system level harmonic assessment were categorised as Scenario 1 and Scenario 2. Particularly, Scenario 1 considered the SSES converters as the only source of harmonic emissions thus disregarding any contributions from customer non-linear loads such as heat pumps, electric vehicles etc. However, for Scenario 2, both SSES and PV converters harmonics and the contributions from other harmonic generating sources were considered in the simulation. The data used for the analysis were all obtained from the field measurements previously described in Section IV.

The simulated results showed that the harmonic injections from the SSESs alone (Scenario 1) did meet the G5/4-1 limits at the secondary side of the substation transformer even for 100% SSESs penetration. However, when the other harmonic generating sources (nonlinear loads like electric vehicle charger, LED lamps and uninterruptible power supply etc) were considered (Scenario 2), the 3rd harmonics was observed to be exceeded. The result is as shown in Table 2.

TABLE 2. Assessing voltage harmonic compliance with EREC G5/4-1.

h	Distortion-Scenario 1	Distortion-Scenario 2	Limit
2	0.0567	0.1889	1.6
3	0.8514	4.1094	4.0
4	0.1171	0.4617	1.0
5	1.5660	2.1237	4.0
6	0.0745	0.2212	0.5
7	0.6894	1.3707	4.0

It was observed that despite the relatively higher 3rd harmonic limit, the THD was less than the 5% limit (4.9% in the test case). Nevertheless, it was realised that downstream the feeder, the voltage THD was significantly higher - as high as 6.3% and higher individual harmonic distortions (IHDs) were also noticed. The expressions for calculating the harmonic performance indices (THD and IHD) are provided in the Appendix.

VI. CONCLUSION

In this paper, it has been verified through field trial on a UK distribution system that there exists a strong case for leveraging on customer-owned SSES units for improvement of the DNO's systems operations. This is especially in the context of peak demand reduction and mitigation of power back-feed into the grid, thus deferring investments on network expansions. Specifically, the evening peak demand of the DNO's network was reduced by up to 60% through smart control of the distributed customer-owned SSESs. Additionally, it was shown that the type-tested SSESs used in the field trials did not pose any significant power-quality related risks to the network. It was also realised that where EREC G83 and G5/4-1 power-quality statutory limits were violated as noticed in some field measurement data, other nonlinear loads were mainly responsible. Having proven practically the flexibility services derivable from the coordinated control of SSESs, the authors recommend that DNO's develop appropriate reward scheme for the use of customer-owned SSESs for flexibility support services in modern smart low voltage networks.

APPENDIX

Network data are as provided below:

- **Service cable**
  $30m \times 35mm^2$ Combined Neutral and Earth (CNE) cable to each customer
  $0.851 + j0.041\Omega/km$(phase)
  $0.90 + j0.041\Omega/km$(neutral)
- **Feeder cable**
- Section A of LV feeder
  $150m \times 185mm^2$, 415V CNE cable
  $0.164 + j0.074\Omega/km$(phase)
  $0.164 + j0.014\Omega/km$(neutral)
- Section B of LV feeder
  $150m \times 95mm^2$, 415V CNE cable
  $0.32 + j0.075\Omega/km$(phase)
  $0.164 + j0.016\Omega/km$(neutral)
- **Transformer**
  500kVA, 11/0.433kV
  4 outgoing, 3-phase feeders
  5% impedance
  Winding arrangement - Dy11
  Reactance to resistance ($\frac{X}{R}$) ratio = 15
  After-diversity-maximum-demand (ADMD) per feeder = 125kVA

A. DEFINITION

The definitions are based on [28].

$$A_{11} = B_{mm} - \left(\frac{Q_m^*\left(V_{r_m}^2 - V_{i_m}^2\right) - 2V_{r_m}V_{i_m}P_m^*}{|V_m|^4}\right) \tag{6}$$

$$A_{12} = A_{21} = G_{mm} - \left(\frac{P_m^*\left(V_{r_m}^2 - V_{i_m}^2\right) + 2V_{r_m}V_{i_m}Q_m^*}{|V_m|^4}\right) \tag{7}$$

$$A_{11} = -B_{mm} - \left(\frac{Q_m^*\left(V_{r_m}^2 - V_{i_m}^2\right) - 2V_{r_m}V_{i_m}P_m^*}{|V_m|^4}\right) \tag{8}$$

$$V_m - \sqrt{V_{r_m}^2 + V_{i_m}^2} = 0 \tag{9}$$

$$\begin{aligned} Q_m^* &= Q_{g(m)}^* - Q_{0(m)}a_q \\ P_m^* &= P_{g(m)}^* - P_{0(m)}a_p \end{aligned} \tag{10}$$

B. HARMONIC ASSESSMENT INDICES

$$\begin{aligned} IHD_{I_h} &= \frac{I_h}{I_1} \times 100\% \\ THD_{I_h} &= \frac{\sqrt{\sum_{h=2}^{H} I_h^2}}{I_1} \times 100\% \\ IHD_{V_h} &= \frac{V_h}{V_1} \times 100\% \\ THD_{V_h} &= \frac{\sqrt{\sum_{h=2}^{H} V_h^2}}{V_1} \times 100\% \end{aligned} \tag{11}$$

ACKNOWLEDGMENT

The authors would like to appreciate Mr. Tobi Babalola and Ms. Ismini Dimitriadou of UK Power Networks, for their supports during the project. Also, thanks to industry partners (Green Running Limited and Powervault Limited) for assisting with field monitoring and acquisition of measurement data. A. Majumdar was with Imperial when he participated in this technical work.

REFERENCES

[1] *Department of Energy and Climate Change, Performance and Impact of the Feed-in Tariff Scheme: Review of Evidence*. Accessed: Jan. 25, 2019. [Online]. Available: https://assets.publishing.service.gov.uk/government/uploads/system/uploads/attachment_data/file/456181/FIT_Evidence_Review.pdf
[2] *Review of the Feed-in Tariff Scheme*. Accessed: Jul. 24, 2019. [Online]. Available: https://assets.publishing.service.gov.uk/government/uploads/system/uploads/attachment_data/file/487300/FITs_Review_Govt_response_Final.pdf
[3] F. Muhammad-Sukki, R. Ramirez-Iniguez, A. B. Munir, S. H. M. Yasin, S. H. Abu-Bakar, S. G. McMeekin, and B. G. Stewart, "Revised feed-in tariff for solar photovoltaic in the United Kingdom: A cloudy future ahead?" *Energy Policy*, vol. 52, pp. 832–838, Oct. 2012.
[4] *The Energy Storage Market in Germany*. Accessed: Jun. 14, 2018. [Online]. Available: https://www.gtai.de/GTAI/Content/EN/Invest/_SharedDocs/Downloads/GTAI/Fact-sheets/Energy-environmental/fact-sheet-energy-storage-market-germany-en.pdf
[5] M. J. E. Alam, K. M. Muttaqi, and D. Sutanto, "Mitigation of rooftop solar PV impacts and evening peak support by managing available capacity of distributed energy storage systems," *IEEE Trans. Power Syst.*, vol. 28, no. 4, pp. 3874–3884, Nov. 2013.
[6] M. Bahadornejad and N. Nair. *Solar PV, Battery Storage and Low Voltage Distribution Network*. Accessed: Jan. 15, 2019. [Online]. Available: https://wiki.auckland.ac.nz/download/attachments/88902304/PV_Battery_White%20Paper_%20October_2013.pdf?version1&modificationDate1415755849000&api̅v2
[7] C. Gonzalez, J. Geuns, S. Weckx, T. Wijnhoven, P. Vingerhoets, T. De Rybel, and J. Driesen, "LV distribution network feeders in Belgium and power quality issues due to increasing PV penetration levels," in *Proc. 3rd IEEE PES Innov. Smart Grid Technol. Eur. (ISGT Eur.)*, Oct. 2012, pp. 1–8.
[8] J. D. Watson, D. Santos-Martin, S. Lemon, A. R. Wood, A. J. Miller, and N. R. Watson, "Impact of solar photovoltaics on the low-voltage distribution network in New Zealand," *IET Gener., Transmiss. Distrib.*, vol. 10, no. 1, pp. 1–9, Jan. 2016.
[9] *Engineering Recommendation G83/1-Recommendations for the Connection of Small-Scale Embedded Generators (Up to 16a Per Phase) in Parallel With Public Low-Voltage Distribution Networks*, Energy Netw. Assoc., London, U.K., 2003.
[10] *International Energy Agency, Overcoming PV Grid Issues in the Urban Areas*. Accessed: May 14, 2018. [Online]. Available: http://www.iea-pvps-task10.org/IMG/pdf/rep10_06.pdf
[11] O. S. Nduka and B. C. Pal, "Harmonic domain modeling of PV system for the assessment of grid integration impact," *IEEE Trans. Sustain. Energy*, vol. 8, no. 3, pp. 1154–1165, Feb. 2017.

[12] O. S. Nduka and B. C. Pal, "Quantitative evaluation of actual loss reduction benefits of a renewable heavy DG distribution network," *IEEE Trans. Sustain. Energy*, vol. 9, no. 3, pp. 1384–1396, Jul. 2018.
[13] X. Liu, A. Aichhorn, L. Liu, and H. Li, "Coordinated control of distributed energy storage system with tap changer transformers for voltage rise mitigation under high photovoltaic penetration," *IEEE Trans. Smart Grid*, vol. 3, no. 2, pp. 897–906, Jun. 2012.
[14] Y. Riffonneau, S. Bacha, F. Barruel, and S. Ploix, "Optimal power flow management for grid connected PV systems with batteries," *IEEE Trans. Sustain. Energy*, vol. 2, no. 3, pp. 309–320, Jul. 2011.
[15] D. Alexander and J. Wyndham, "Harnessing voltage regulation services behind the meter: Challenges to deployment," in *Proc. Int. Conf. Innov. Appl. Energy (IAPE)*, 2019.
[16] J. Barros. *Engineering Design Standard, Eds 08-5010, Energy Storage, UK Power Networks*. Accessed: Jun. 3, 2018. [Online]. Available: http://library.ukpowernetworks.co.uk/library/asset/9dd7b8d4-fd6d-491d-aa18-196ffe25863P/EDS+08-5010+Energy+Storage.pdf
[17] S. Daniel. *Distributed (Home) Energy Storage and Aggregated Grid Services*. Accessed: Jun. 3, 2018. [Online]. Available: http://www.energy.ox.ac.uk/wordpress/wp-content/uploads/2016/12/Daniel-Moixa.pdf
[18] N. T. M. Dale, R. Hey, and P. Swift. *Project Sola Bristol, Closedown Report, Western Power Distribution*. Accessed: Mar. 12, 2019. [Online]. Available: https://www.westernpower.co.uk/docs/Innovation/Closed-projects/SoLa-Bristol/SoLa-Bristol-Closedown-Report-FINAL-090616-CLEAN.aspx
[19] G. E. M. Coulthard, M. Fila, and R. Potter. *New Thames Valley Vision Learning Outcome Report: LV Network Storage—ESMU Trials*. Accessed: Aug. 3, 2018. [Online]. Available: http://www.thamesvalleyvision.co.uk/wp-content/uploads/2017/05/NTVV-Learning-Outcome-Report-LV-Network-Storage-ESMU-Trials.pdf
[20] A. Services. *Demand Management Case Study—Residential Battery Storage Trial*. Accessed: Jun. 6, 2018. [Online]. Available: http://www.demandresponse.com.au/articles/2016/04/ausnet-services-publishes-results-oftheir-residential-battery-storage-trial
[21] O. Nduka, L. Kunjumuhammed, B. Pal, I. Dimitriadou, and B. Shahnavaz, "Domestic energy storage and control project—Network impact assessment report," to be published.
[22] P. Consulting. *Aggregators Barriers and External Impacts: A Report by PA Consulting*. Accessed: Jun. 6, 2018. [Online]. Available: https://www.ofgem.gov.uk/system/files/docs/2016/07/aggregators-barriers_and_external_impacts_a_report_by_pa_consulting_0.pdf
[23] *Engineering Recommendation G100—Technical Requirements for Customer Export Limiting Schemes*, Energy Netw. Assoc., London, U.K., 2017.
[24] *G59-Recommendation for the Connection of Generating Plant to the Distribution Systems of Licensed Distribution Network Operators*, Energy Netw. Assoc., London, U.K., 2014.
[25] M. B. Abdullah, "On a robust correlation coefficient," *Statistician*, vol. 39, no. 4, p. 455, 1990.
[26] *15,* 0 *User Manual*, DigSilent Powerfactory, Gomaringen, Germany, 2016.
[27] S. Ingram, S. Probert, and K. Jackson, "The impact of small scale embedded generation on the operating parameters of distribution networks," Dept. Trade Ind., PB Power, London, U.K., Tech. Rep. K/EL/00303/04/01, 2003.
[28] V. Da Costa, N. Martins, and J. Pereira, "Developments in the Newton Raphson power flow formulation based on current injections," *IEEE Trans. Power Syst.*, vol. 14, no. 4, pp. 1320–1326, Nov. 1999.
[29] P. Garcia, J. Pereira, S. Carneiro, V. Da Costa, and N. Martins, "Three-phase power flow calculations using the current injection method," *IEEE Trans. Power Syst.*, vol. 15, no. 2, pp. 508–514, May 2000.
[30] D. Penido, L. Araujo, J. Pereira, P. Garcia, and S. Carneiro, "Four wire Newton-Raphson power flow based on the current injection method," in *Proc. IEEE PES Conf. Power Syst. Conf. Expo.*, Apr. 2005, pp. 239–242.
[31] D. R. R. Penido, L. R. De Araujo, S. Carneiro, J. L. R. Pereira, and P. A. N. Garcia, "Three–phase power flow based on four–conductor current injection method for unbalanced distribution networks," *IEEE Trans. Power Syst.*, vol. 23, no. 2, pp. 494–503, May 2008.
[32] K. Wang, H. Huang, and C. Zang, "Research on time-sharing zip load modeling based on linear bp network," in *Proc. 5th Int. Conf. Intell. Hum.-Mach. Syst. Cybern. (IHMSC)*, vol. 1, Aug. 2013, pp. 37–41.
[33] A. Medina, J. Segundo-Ramirez, P. Ribeiro, W. Xu, K. Lian, G. Chang, V. Dinavahi, and N. Watson, "Harmonic analysis in frequency and time domain," *IEEE Trans. Power Del.*, vol. 28, no. 3, pp. 1813–1821, Jul. 2013.
[34] J.-H. Teng and C.-Y. Chang, "Backward/forward sweep–based harmonic analysis method for distribution systems," *IEEE Trans. Power Del.*, vol. 22, no. 3, pp. 1665–1672, Jul. 2007.
[35] V. Ćuk, W. L. Kling, J. F. Cobben, and P. F. Ribeiro, "Analysis of harmonic current summation based on field measurements," *IET Gener., Transmiss. Distrib.*, vol. 7, no. 12, pp. 1391–1400, Dec. 2013.
[36] *Assessment of Emission Limits for the Connection of Disturbing Installations to LV Power Systems*, Standard IEC 61000-3-14, 2011.
[37] *Electromagnetic Compatibility (EMC)—Part 3-6: Limits-Assessment of Emission Limits for the Connection of Distorting Installations to MV, HV and EHV Power Systems, HV and EHV Power Systems*, Standard IEC 61000-3-6, 2008.

ONYEMA S. NDUKA (Member, IEEE) received the B.Eng. degree in electrical and electronic engineering from the Federal University of Technology, Owerri, Nigeria, in 2011, and the M.Sc. degree in control systems and the Ph.D. degree in electrical engineering from Imperial College London, U.K., in 2014 and 2018, respectively.

He is currently a Postdoctoral Research Associate with the Control and Power Group, Imperial College London. He was a Power Quality Consultant with the UK Power Networks NIA funded project on Domestic Energy Storage and Control (DESC). He is also a COREN Registered Electrical Engineer and a Certified PRINCE2 Practitioner. His research interests include distribution systems and microgrid planning and operation, power quality, power quality state estimation, low-carbon technology (including photovoltaics, small-scale energy storage, and electric vehicles) integration into smart grids and power quality big data analytics.

LINASH P. KUNJUMUHAMMED (Senior Member, IEEE) received the M.S. degree from the IIT Madras, Chennai, India, and the Ph.D. degree from the Imperial College London, U.K., in 2006 and 2012 respectively, all in electrical engineering.

He is currently working as a HVDC Engineer with Mitsubishi Electric Europe BV.

BIKASH C. PAL (Fellow, IEEE) received the B.E.E. degree (Hons.) from Jadavpur University, Calcutta, India, the M.E. degree from the Indian Institute of Science, Bangalore, India, and the Ph.D. degree from Imperial College London, London, U.K., in 1990, 1992, and 1999, respectively, all in electrical engineering.

He is currently a Professor with the Department of Electrical and Electronic Engineering, Imperial College London. His current research interests include renewable energy modeling and control, state estimation, and power system dynamics. He is a Fellow of IEEE for his contribution to power system stability and control. He was an Editor-in-Chief of the IEEE TRANSACTIONS ON SUSTAINABLE ENERGY, from 2012 to 2017 and an Editor-in-Chief of *IET Generation, Transmission and Distribution,* from 2005 to 2012. He is the Vice President Publications of the IEEE Power and Energy Society.

ANKUR MAJUMDAR (Member, IEEE) received the bachelor's degree in electrical engineering and the master's degree in electric power systems from India, and the Ph.D. degree in electric power engineering from Imperial College London, U.K. Before DEPsys, he worked as a Research Engineer with IERC, Ireland and as a Postdoctoral Research Associate with Imperial College London. He has also been a Consultant to UK Power Networks and Powervault in a NIA funded project. He is currently an Research and Development Scientist at DEPsys SA, Switzerland, where he is also involved in power system flexibility and other Research and Development activities. He has published several peer-reviewed journals and conference papers. His research interests are power system flexibility, power quality, power system state estimation, active network management, optimization, and voltage var control of distribution systems. During his professional career, he has become a member of IEEE and IEEE Working Group on Distribution System State Estimation.

YUE YU received the B.Sc. degrees in electrical engineering from the University of Bath, U.K., and also from North China Electric Power University, China, in 2015, and the M.Sc. degree in advanced electrical machines, power electronics and drives from the University of Sheffield, U.K., in 2016. He is currently pursuing the Ph.D. degree with Imperial College London, U.K. His research interest includes modeling, control, and optimization of dc microgrid with integration of electric vehicle fleet.

SUMAN MAITI (Member, IEEE) received the B.E. degree from the Jalpaiguri Government Engineering College, Jalpaiguri, India, in 2002, the master's degree from the Indian Institute of Engineering Science and Technology Shibpur, Howrah, India, in 2004, and the Ph.D. degree from IIT Kharagpur, Kharagpur, India, in 2009, all in electrical engineering.

Since 2009, he has been working with the Research and Development (R&D) Group, ABB (India) Ltd., as an Associate Scientist. In 2014, he joined the Department of Electrical Engineering, IIT Kharagpur, as an Assistant Professor. His research interests include multilevel converters and electric vehicles.

ALI R. AHMADI received the B.Eng. degree (Hons.) in electronic and electrical engineering from University College London and the Ph.D. degree in active network management (ANM) systems from Imperial College London.

He is currently the Senior Power System Development Engineer with UK Power Networks' Smart Grid Development Team. He is also the Scheme Design Lead on Active Network Management, Power Potential and Regional Development Program projects. He leads the company's stream of activities in Advanced Network Modeling. His engineering career has spanned a wide breadth of smart grid themes. He has got extensive experience in design, development and operation of end-to-end control systems for transmission and distribution networks.